

Matrix Isolation Infrared Spectroscopic and Density Functional Theoretical Calculations of the GeO_2^- and GeO_4^- Anions

Mingfei Zhou,* Limin Shao, and Lei Miao

Department of Chemistry and Laser Chemistry Institute, Fudan University, Shanghai 200433, P. R. China

Received: January 9, 2002; In Final Form: May 2, 2002

Laser ablated germanium atoms and electrons have been co-deposited with O_2 in excess argon at 11 K. In addition to previously assigned O_4^+ , O_4^- , O_3^- , GeO, and GeO_2 species, GeO_2^- and GeO_4^- anions were produced and identified from isotopic splittings on their matrix infrared spectra and from density functional theory calculations. In contrast to linear GeO_2 , the GeO_2^- anion is bent with a bond angle estimated to be $134 \pm 2^\circ$ based on the isotopic ν_3 vibrational frequencies. The GeO_4^- anion was predicted to have nonplanar C_s structure with significantly high vertical detachment energy.

1. Introduction

The study of germanium oxides is of fundamental interest. There have been some experimental and theoretical studies on the reaction products formed by germanium and oxygen in the gas phase and in solid matrices. The $(\text{GeO})_n$ molecular oxides with $n = 1-4$ (starting from evaporated GeO) have been formed and observed in an argon matrix by Ogden and co-workers.¹ The structures of these germanium oxides were determined by the experimentally obtained IR absorption spectra. The GeO_2 molecule was later produced in nitrogen and krypton matrices by Bos et al. and in an argon matrix by Andrews and co-workers via germanium atom and molecular oxygen reaction.²⁻⁴ The $(\text{GeO})_n$ clusters were reinvestigated by Zumbusch and Schnökel using IR and Raman spectroscopy as well as quantum chemical calculations.⁵ More recently, the structures, bonding, and reactivities of molecular germanium oxides were studied by Johnson and Panas using density functional methods.⁶

In contrast to the well-characterized neutral germanium oxide molecules, the germanium oxide anion species have gained much less attention. The photoelectron spectra of the GeO_2^- and Ge_2O_3^- anions have been studied by Wang et al. in the gas phase.⁷ All the spectra showed broad photodetachment features, suggesting that there is considerable geometry change between the anion and the neutral. The vertical detachment energy was determined to be 2.93 eV for GeO_2^- . The structure and energy of GeO_2^- has also been calculated by density functional theory.⁶ In contrast to the linear GeO_2 , the GeO_2^- anion was predicted to be bent with C_{2v} symmetry. The adiabatic electron affinity of GeO_2 and the vertical detachment energy of GeO_2^- were calculated to be 2.24 and 3.21 eV, respectively, in good agreement with experimental values.⁷ To our knowledge, there is no experimental report on vibrational spectra of germanium oxide anions. In this paper, we report the vibrational spectra and quantum chemical calculations of the GeO_2^- and GeO_4^- anions produced by co-condensation of laser ablated germanium atoms and electrons with molecular oxygen in excess argon.

2. Experimental and Computational Methods

The experimental setup for pulsed laser ablation and matrix infrared spectroscopic investigation has been described in detail

previously.⁸ Briefly, the 1064 nm fundamental of a Nd:YAG laser (20 Hz repetition rate and 8 ns pulse width) was used as the ablation laser. The ablated germanium atoms and electrons were co-deposited with O_2 in excess argon onto a 11 K CsI window for 1 h at a rate of approximately 4 mmol/h. Typically, 5–10 mJ/pulse laser power was used. O_2 (Shanghai BOC, 99.95%) and $^{18}\text{O}_2$ (Cambridge Isotope Laboratories, 99%) were used in different experiments. Infrared spectra were recorded on a Bruker IFS 113v spectrometer at 0.5 cm^{-1} resolution using a DTGS detector. Matrix samples were annealed at different temperatures and were subjected to broadband photolysis using a high-pressure mercury arc lamp.

Quantum chemical calculations were performed to predict the structures and vibrational frequencies of the reaction products using the Gaussian 98 program.⁹ Becke's three-parameter hybrid functional with additional correlation corrections due to Lee, Yang, and Parr was utilized.^{10,11} Additional comparison CCSD-(T) calculations were done on GeO_2 and GeO_2^- as well. The 6-311+G(d) basis sets were used for Ge and O atoms.^{12,13} Geometries were fully optimized. The vibrational frequencies were calculated with analytic second derivatives, and zero point vibrational energies (ZPVE) were derived.

3. Results and Discussions

A. Infrared Spectra. The present experiments employed low ablation laser energy, typically 5 to 10 mJ/pulse, and the germanium atom concentration was estimated to be about 1 order of magnitude lower than the O_2 concentration. At such experimental conditions, the possibility for the formation of dimetal or multimetal species is rather small. As will be mentioned, the spectrum on sample deposition at 11 K was dominated by GeO_2 and GeO absorptions, and no obvious multi-germanium oxide absorption was observed, even after 25 to 28 K annealing. Of particular importance here, low laser energy ablation experiments favored the stabilization and trapping of charged species in solid argon matrix.

Figure 1 shows the spectra in the 1080–780 cm^{-1} region from co-deposition of laser ablated germanium with 1.0% O_2 in argon, and the product absorptions are listed in Table 1. In addition to absorptions due to O_3 (1039.5 cm^{-1}), O_3^- (804.1 cm^{-1}), O_4^- (953.8 cm^{-1}), and O_4^+ (1118.7 cm^{-1}) that are common to other metal reactions with O_2 ,¹⁴⁻¹⁶ the GeO and

* Corresponding author. E-mail: mzfzhou@fudan.edu.cn. Fax: +86-21-65643532.

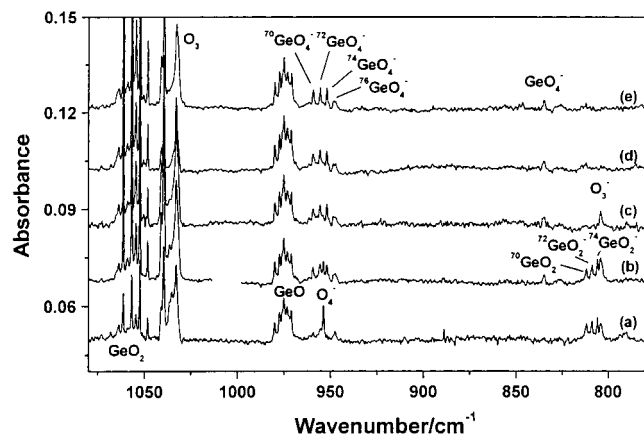


Figure 1. Infrared spectra in the 1080–780 cm^{-1} region from co-deposition of laser ablated Ge with 1.0% O_2 in argon. (a) 1 h sample deposition at 11 K, (b) 25 K annealing, (c) 20 min $\lambda > 290$ nm photolysis, (d) 20 min full arc photolysis, and (e) 28 K annealing.

TABLE 1: Infrared Absorptions (cm^{-1}) from Co-deposition of Laser Ablated Ge Atoms with O_2 in Excess Oxygen at 11 K

$^{16}\text{O}_2$	$^{18}\text{O}_2$	R(16/18)	assignment
1118.7	1056.2	1.0592	O_4^+
1061.2	1020.4	1.0400	$^{70}\text{GeO}_2$
1056.6	1015.6	1.0404	$^{72}\text{GeO}_2$
1054.4	1013.4	1.0405	$^{73}\text{GeO}_2$
1052.2	1011.1	1.0406	$^{74}\text{GeO}_2$ (asy-OGeO str.)
1048.1	1006.8	1.0410	$^{76}\text{GeO}_2$
1039.5	982.2	1.0583	O_3
1032.9	976.1	1.0582	O_3 site
980.0	934.7	1.0485	^{70}GeO
977.5	932.1	1.0487	^{72}GeO
975.1	929.6	1.0489	^{74}GeO
959.6	921.4	1.0415	$^{70}\text{GeO}_4^-$
955.7	917.3	1.0419	$^{72}\text{GeO}_4^-$
953.8	901.8	1.0577	O_4^-
952.0	913.5	1.0421	$^{74}\text{GeO}_4^-$ (asy-OGeO str.)
948.5	909.8	1.0425	$^{76}\text{GeO}_4^-$
834.8	789.3	1.0576	GeO_4^- (sym-OGeO str.)
811.8	778.9	1.0422	$^{70}\text{GeO}_2^-$
808.7	775.7	1.0425	$^{72}\text{GeO}_2^-$
805.8	772.7	1.0428	$^{74}\text{GeO}_2^-$ (asy-OGeO str.)
804.1	759.1	1.0593	O_3^-

GeO_2 absorptions and a set of new bands at 805.8, 808.7, and 811.8 cm^{-1} were observed after sample deposition at 11 K. Sample annealing to 25 K decreased the O_4^+ and O_4^- absorptions and increased the GeO_2 and O_3 absorptions. Meanwhile, a family of new absorptions at 948.5, 952.0, 955.7, and 959.6 cm^{-1} , together with a 834.8 cm^{-1} band, were produced. Mercury lamp photolysis with a 290 nm long-wavelength pass filter destroyed the O_4^- and O_4^+ absorptions as well as the 805.8, 808.7, and 811.8 cm^{-1} absorptions with little effect on the other bands. Subsequent full arc photolysis wiped out the O_3^- absorption. The new bands at 948.5–959.6 and 834.8 cm^{-1} exhibited no obvious change on full arc photolysis or on further 28 K annealing.

Experiments were done using different O_2 concentrations. Figure 2 shows the spectra in the 1000–780 cm^{-1} region using 2% O_2 in argon. Compared to the 1% O_2 experiment shown in Figure 1, the absorptions at 834.8, 948.5, 952.0, 955.7, and 959.6 cm^{-1} were presented on sample deposition and increased on annealing in 2% experiment.

One experiment was done with 1.5% $^{18}\text{O}_2$ in argon, and the spectra in the 1040–740 cm^{-1} region are shown in Figure 3. All the product absorptions were shifted as listed in Table 1. Experiment was also performed with a 0.5% $^{16}\text{O}_2 + 1.0\%$

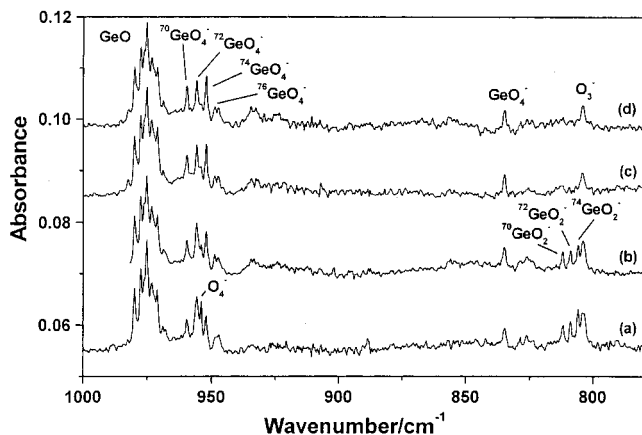


Figure 2. Infrared spectra in the 1000–780 cm^{-1} region from co-deposition of laser ablated Ge with 2.0% O_2 in argon. (a) 1 h sample deposition at 11 K, (b) 25 K annealing, (c) 20 min $\lambda > 290$ nm photolysis, and (d) 28 K annealing.

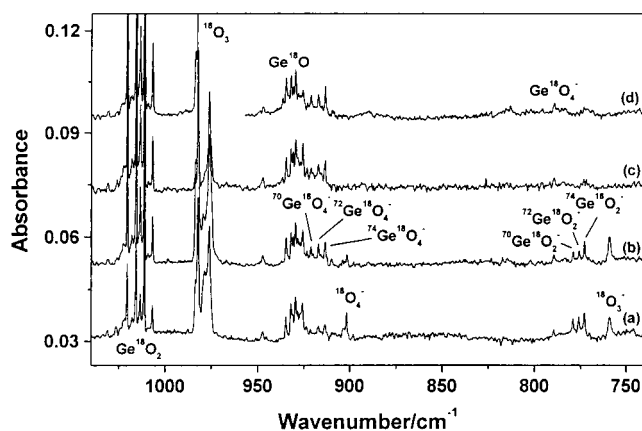


Figure 3. Infrared spectra in the 1040–740 cm^{-1} region from co-deposition of laser ablated Ge with 1.5% $^{18}\text{O}_2$ in argon. (a) 1 h sample deposition at 11 K, (b) 25 K annealing, (c) 20 min full arc photolysis, and (d) 28 K annealing.

$^{16}\text{O}^{18}\text{O} + 0.5\% ^{18}\text{O}_2$ sample, but the spectra for the new product absorptions were too weak to be observed due to isotopic dilutions.

B. GeO, GeO_2 . Germanium monoxide and dioxide molecules have been well characterized by matrix isolation IR spectroscopy.^{1–4} Based on previous reports, the absorptions at 975.1, 977.5, and 980.0 cm^{-1} are assigned to the ^{74}GeO , ^{72}GeO , and ^{70}GeO molecules, and the bands at 1048.1, 1052.2, 1054.4, 1056.6, and 1061.2 cm^{-1} are assigned to the antisymmetric stretching vibrations of isotopic GeO_2 molecules.^{3,4} In agreement with previous calculations,⁶ GeO_2 was found to be linear. The Ge–O bond length was predicted to be 1.629 Å with B3LYP and 1.645 Å with CCSD(T). The antisymmetric stretching vibration for $^{74}\text{GeO}_2$ was calculated at 1039.4 cm^{-1} , slightly lower than the experimental value. As listed in Table 4, the calculated germanium and oxygen isotopic frequency ratios are very close to the experimental values.

C. GeO_2^- . The bands at 805.8, 808.7, and 811.8 cm^{-1} appeared on sample deposition. Their relative intensities matched natural isotopic abundance of ^{74}Ge , ^{72}Ge , and ^{70}Ge , which clearly indicated one Ge atom involvement. These bands shifted to 772.7, 775.7, and 778.9 cm^{-1} in the $^{18}\text{O}_2$ experiment. The isotopic $^{16}\text{O}/^{18}\text{O}$ ratios 1.0428, 1.0425, and 1.0422 indicated that these bands are due to antisymmetric OGeO stretching vibrations. These bands were destroyed on $\lambda > 290$ nm photolysis and were not observed in previous thermal germanium atom

TABLE 2: Calculated (B3LYP/6-311+G(d)) Isotopic Vibrational Frequencies (cm^{-1}) and Intensities (in parentheses, km/mol) for GeO_2 and GeO_2^-

	ν_1	ν_2	ν_3
$^{74}\text{Ge}^{16}\text{O}_2$	864.7(0)	203.8(80)	1039.4(82)
$^{74}\text{Ge}^{18}\text{O}_2$	815.1(0)	195.7(74)	998.2(75)
$^{72}\text{Ge}^{16}\text{O}_2$	864.7(0)	204.7(80)	1043.8(82)
$^{74}\text{Ge}^{16}\text{O}_2^-$	746.4(21)	238.0(37)	781.9(131)
$^{74}\text{Ge}^{18}\text{O}_2^-$	706.4(19)	222.7(32)	749.2(117)
$^{72}\text{Ge}^{16}\text{O}_2^-$	747.0(21)	238.8(37)	784.8(131)

TABLE 3: Calculated (B3LYP/6-311+G(d)) Isotopic Vibrational Frequencies (cm^{-1}) and Intensities (in parentheses, km/mol) for the GeO_4^- Anion

$^{74}\text{Ge}^{16}\text{O}_4^-$	1167.9(6), 936.1(162), 822.0(46), 445.5(62), 273.8(90), 238.6(38), 215.7(10), 150.4(10), 29.9(1)
$^{74}\text{Ge}^{18}\text{O}_4^-$	1101.0(5), 897.8(148), 776.8(44), 423.9(59), 262.4(79), 229.5(34), 204.8(9), 142.3(8), 28.2(1)
$^{72}\text{Ge}^{16}\text{O}_4^-$	1167.9(6), 939.7(163), 822.5(47), 446.4(63), 274.8(90), 239.7(38), 216.1(10), 150.6(10), 29.9(1)

TABLE 4: Comparison of the Observed and Calculated Isotopic Frequency Ratios of the GeO_2 , GeO_2^- , and GeO_4^- Anions

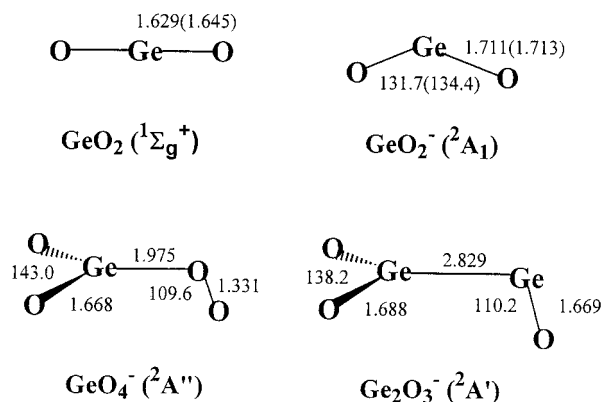
	$^{16}\text{O}/^{18}\text{O}$ (^{74}Ge)		$^{72}\text{Ge}/^{74}\text{Ge}$ (^{16}O)		$^{70}\text{Ge}/^{74}\text{Ge}$ (^{16}O)		
	exp.	calc.	exp.	calc.	exp.	calc.	
GeO_2 (ν_3)	1.0406	1.0413	1.0042	1.0042	1.0086	1.0087	
GeO_2^- (ν_3)	1.0428	1.0436	1.0036	1.0037	1.0074	1.0075	
GeO_4^-	asy- OGeO	1.0421	1.0427	1.0039	1.0038	1.0080	1.0080
	sym- OGeO	1.0576	1.0582		1.0006		1.0011

and oxygen reaction experiments, suggesting an anion assignment. The mixed isotopic structures in the $^{16}\text{O}_2 + ^{16}\text{O}^{18}\text{O} + ^{18}\text{O}_2$ experiments were too weak to be observed due to isotopic dilution. These bands were initial product absorptions in different O_2 concentration experiments, so only two O atoms are most likely involved. Therefore, the 805.8, 808.7, and 811.8 cm^{-1} bands are assigned to the antisymmetric stretching vibrations of the isotopic GeO_2^- anions. The $^{76}\text{GeO}_2^-$ absorption was overlapped by the O_3^- absorption at 804.1 cm^{-1} . The $^{73}\text{GeO}_2^-$ absorption was much weaker and was not observed.

The anion assignment was supported by theoretical calculations. In contrast to the linear GeO_2 molecule, DFT calculation predicted a bent GeO_2^- anion with a $^2\text{A}_1$ ground state. As shown in Figure 4, the Ge–O bond distance and the bond angle were predicted to be 1.711 Å and 131.7° (B3LYP) or 1.713 Å and 134.4° (CCSD(T)). The antisymmetric O^{74}GeO stretching vibration was predicted at 781.9 cm^{-1} , which is 23.9 cm^{-1} lower than the observed value. We note that B3LYP calculation also predicted the antisymmetric stretching vibration of GeO_2 to be 12.8 cm^{-1} lower than observed. Although the vibrational frequency was predicted to be slightly low, the calculated germanium and oxygen isotopic ratios are in excellent agreement with experimental values, as listed in Table 4. The symmetric stretching mode was predicted at 746.4 cm^{-1} with about 16% intensity of the antisymmetric mode. This mode was not observed in our experiments.

The isotopic antisymmetric OGeO stretching vibrational frequencies for GeO_2^- provide a basis for calculation of the valence angle of the GeO_2^- anion.^{17–19} The upper limit of OGeO bond angle was estimated to be 139°, and the low limit was estimated to be 129°. A determination of $134 \pm 2^\circ$ is proposed for the OGeO bond angle, which is in excellent agreement with the calculated bond angle (131.7° from B3LYP and 134.4° from CCSD(T)) for GeO_2^- .

The GeO_2^- anion has been studied by Wang et al. using anion photoelectron spectroscopy.⁷ The photoelectron spectrum of

**Figure 4.** Calculated (B3LYP/6-311+G(d)) structures of the GeO_2 , GeO_2^- , GeO_4^- , and Ge_2O_3^- anions. (bond length in Å, bond angle in degree, CCSD(T) values are listed in the parenthesis.)

GeO_2^- was obtained. The spectrum represented photodetachment transitions from the ground state of the GeO_2^- anion to the GeO_2 neutral states. The spectrum is quite broad, suggesting that there is large geometry change from the anion to the neutral, which was supported by our DFT calculations. As shown in Figure 4, the GeO_2 neutral is linear while the GeO_2^- anion is bent with a bond angle around 130°. The bond length of GeO_2^- (1.711 Å at the B3LYP level of theory) elongated by about 0.082 Å compared with that of the GeO_2 neutral. The adiabatic electron affinity of GeO_2 and the vertical detachment energy of GeO_2^- were experimentally determined to be 2.50 and 2.93 eV, respectively. These two values were calculated to be 2.37 and 3.28 eV at the B3LYP/6-311+G(d) level of theory.

D. GeO_4^- . A family of bands from 959.6 to 948.5 cm^{-1} exhibited the intensity distribution for natural abundance germanium isotopes and clearly indicated one germanium atom involvement. These bands shifted to 921.4–909.8 cm^{-1} with $^{18}\text{O}_2$ and gave $^{16}\text{O}/^{18}\text{O}$ isotopic ratios ranging from 1.0415 to 1.0425. The isotopic ratios are characteristic of antisymmetric OGeO stretching vibrations of bent GeO_2 . A weaker band at 834.8 cm^{-1} exhibited the same annealing and photolysis behavior with the 959.6–948.5 cm^{-1} bands. Although the germanium isotopic splittings could not be resolved for the 834.8 cm^{-1} band, the isotopic $^{16}\text{O}/^{18}\text{O}$ ratio of 1.0576 indicated that this band is due to a symmetric OGeO stretching vibration. The aforementioned bands were not observed in previous thermal experiments, suggesting that they be also due to charged species. Compared to the GeO_2^- absorptions, these bands showed more O_2 concentration dependence. They appeared after the GeO_2^- absorptions on annealing in lower O_2 concentration experiments. Therefore, a GeO_x^- species with $x \geq 3$ should be considered.

Assignment of these bands to isotopic GeO_4^- anions first came into mind. Previous studies reported by Jacox and co-workers showed that when a $\text{Ne}/\text{CO}_2/\text{O}_2 = 200:1:1$ mixture was co-deposited at 5 K with a beam of neon atoms that have been excited, the CO_4^- anion was formed.²⁰ The CO_4^- anion is quite stable with a photodecomposition threshold near 260 nm. Present DFT calculations confirmed the GeO_4^- anion assignment. As shown in Figure 4, the GeO_4^- anion has a nonplanar C_s structure with the Ge–OO plane perpendicular to the OGeO plane. The antisymmetric and symmetric O^{74}GeO stretching vibrations were predicted at 936.1 and 822.0 cm^{-1} with 162:46 km/mol relative intensities. Of particular importance, the calculated germanium and oxygen isotopic ratios are in excellent agreement with the experimental values (Table 4). For the symmetric OGeO stretching mode, the ^{72}Ge and ^{74}Ge splittings were predicted to be only about 0.5 cm^{-1} . Apparently, the germanium isotopic

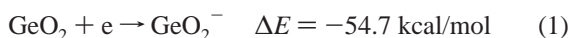
splittings could not be resolved for this mode with 0.5 cm^{-1} spectrometer resolution. The O–O stretching vibration was calculated at 1167.9 cm^{-1} with very low intensity (6 km/mol), and was not observed.

The structure and bonding of the GeO_4^- anion is quite similar to that of the CO_4^- , C_2O_3^- , and CO_2NO^- anions.^{20–22} The Ge–OO bond is approximately a single bond with bond distance calculated to be 1.975 \AA at the B3LYP level. Mulliken population analysis showed that the electron spin density is concentrated on the O atoms of the O_2 moiety (64% in terminal O atom, 36% in another O atom), while the charge density is about equal in both the GeO_2 and O_2 units (0.49 e versus 0.51 e). It is interesting to note that the Ge=O bond distance in GeO_4^- is almost equal to the mean value of the GeO_2 and GeO_2^- bond distances.

Our DFT calculations predicted that the GeO_4^- anion is stable by 65.6 kcal/mol with respect to $\text{GeO}_2 + \text{O}_2^-$, and is stable by 24.9 kcal/mol with respect to $\text{GeO}_2^- + \text{O}_2$. The vertical detachment energy was predicted to be 110.0 kcal/mol (4.77 eV), significantly higher than that of the GeO_2^- anion. The invariance of the GeO_4^- absorptions under full arc photolysis ($\lambda > 250\text{ nm}$) conditions also indicated that this anion has high vertical detachment energy.

Wang and co-workers have also measured photoelectron spectrum of the Ge_2O_3^- anion.⁷ The spectrum is consistent with only one isomer. Our DFT calculations predicted the Ge_2O_3^- anion to have nonplanar C_s structure, as also shown in Figure 4. Recent DFT calculations indicated that two types of structures are possible for Ge_2O_3 neutral.⁶ The planar GeO_2GeO structure with C_{2v} symmetry is more stable than the GeO_3Ge structure with trigonal bipyramid D_{3h} symmetry. Apparently, the anion structure is quite different with the neutral structures. Neither the Ge_2O_3^- anion nor the Ge_2O_3 neutral was observed in our experimental conditions.

The GeO_2^- anions were formed by electron capture of the GeO_2 neutrals, i.e., reaction 1, which was calculated to be exothermic by 54.7 kcal/mol . The GeO_4^- anion absorptions increased on annealing, which suggested that the GeO_4^- anions were most probably formed by ion–molecule reactions 2 and 3 in argon matrix:



4. Conclusions

Laser ablated germanium atoms and electrons have been reacted with O_2 in excess argon at 11 K . In addition to previously assigned O_4^+ , O_4^- , O_3^- , GeO , and GeO_2 species, the GeO_2^- and GeO_4^- anions were produced and identified from

isotopic splittings on their matrix infrared spectra and from density functional theory calculations. Photosensitive absorptions at 805.8 , 808.7 , and 811.8 cm^{-1} are assigned to the antisymmetric OGeO stretching vibrations of the $^{74}\text{GeO}_2^-$, $^{72}\text{GeO}_2^-$, and $^{70}\text{GeO}_2^-$ anions. In contrast to linear GeO_2 , the GeO_2^- anion is bent with a bond angle estimated to be $134 \pm 2^\circ$ based on the isotopic ν_3 vibrational frequencies. New absorptions at 948.5 to 959.6 and 834.8 cm^{-1} are assigned to the antisymmetric and symmetric OGeO stretching vibrations of the isotopic GeO_4^- anions. The GeO_4^- anion was predicted to have nonplanar C_s structure with significantly high vertical detachment energy.

Density functional theory using the B3LYP functional predicted vibrational frequencies of the germanium oxide neutrals and anions systematically slightly lower than the experimental values, but the calculated isotopic frequency ratios in excellent agreement with experimental values.

Acknowledgment. This work is supported by NSFC (Grant No. 20125033).

References and Notes

- Ogden, J. S.; Ricks, M. J. *J. Chem. Phys.* **1970**, *52*, 352.
- Bos, A.; Ogden, J. S.; Ogree, L. *J. Phys. Chem.* **1974**, *78*, 1763.
- Hassanzadeh, P.; Andrews, L. *J. Phys. Chem.* **1992**, *96*, 6181.
- Andrews, L.; McCluskey, M. *J. Mol. Spectrosc.* **1992**, *154*, 223.
- Zumbusch, A.; Schnöckel, H. *J. Chem. Phys.* **1998**, *108*, 8092.
- Johnson, J. R. T.; Panas, I. *Chem. Phys.* **1999**, *249*, 273.
- Wang, L. S.; Wu, H. B.; Desai, S. R.; Fan, J. W.; Colson, S. D. *J. Phys. Chem.* **1996**, *100*, 8697.
- Chen, M. H.; Wang, X. F.; Zhang, L. N.; Yu, M.; Qin, Q. *Z. Chem. Phys.* **1999**, *242*, 81.
- Frisch, M. J.; Trucks, G. W.; Schlegel, H. B.; Scuseria, G. E.; Robb, M. A.; Cheeseman, J. R.; Zakrzewski, V. G.; Montgomery, J. A., Jr.; Stratmann, R. E.; Burant, J. C.; Dapprich, S.; Millam, J. M.; Daniels, A. D.; Kudin, K. N.; Strain, M. C.; Farkas, O.; Tomasi, J.; Barone, V.; Cossi, M.; Cammi, R.; Mennucci, B.; Pomelli, C.; Adamo, C.; Clifford, S.; Ochterski, J.; Petersson, G. A.; Ayala, P. Y.; Cui, Q.; Morokuma, K.; Malick, D. K.; Rabuck, A. D.; Raghavachari, K.; Foresman, J. B.; Cioslowski, J.; Ortiz, J. V.; Baboul, A. G.; Stefanov, B. B.; Liu, G.; Liashenko, A.; Piskorz, P.; Komaromi, I.; Gomperts, R.; Martin, R. L.; Fox, D. J.; Keith, T.; Al-Laham, M. A.; Peng, C. Y.; Nanayakkara, A.; Gonzalez, C.; Challacombe, M.; Gill, P. M. W.; Johnson, B.; Chen, W.; Wong, M. W.; Andres, J. L.; Gonzalez, C.; Head-Gordon, M.; Replogle, E. S.; Pople, J. A. *Gaussian 98*, revision A.7; Gaussian, Inc.: Pittsburgh, PA, 1998.
- Lee, C.; Yang, E.; Parr, R. G. *Phys. Rev. B* **1988**, *37*, 785.
- Becke, A. D. *J. Chem. Phys.* **1993**, *98*, 5648.
- McLean, A. D.; Chandler, G. S. *J. Chem. Phys.* **1980**, *72*, 5639.
- Krishnan, R.; Binkley, J. S.; Seeger, R.; Pople, J. A. *J. Chem. Phys.* **1980**, *72*, 650.
- Jacox, M. E.; Thompson, W. E. *J. Chem. Phys.* **1994**, *100*, 750.
- Zhou, M. F.; Hacıaloglu, J.; Andrews, L. *J. Chem. Phys.* **1999**, *110*, 9450.
- Andrews, L.; Spiker, R. C. *J. Phys. Chem.* **1972**, *76*, 3208.
- Allavena, M.; Rysnik, R.; White, D.; Calder, V.; Mann, D. E. *J. Chem. Phys.* **1969**, *50*, 3399.
- Green, D. W.; Ervin, K. M. *J. Mol. Spectrosc.* **1981**, *88*, 51.
- Bare, W. D.; Souter, P. F.; Andrews, L. *J. Phys. Chem. A* **1998**, *102*, 8279.
- Jacox, M. E.; Thompson, W. E. *J. Phys. Chem.* **1991**, *95*, 2781.
- Zhou, M. F.; Zhang, L. N.; Chen, M. H.; Qin, Q. *Z. J. Chem. Phys.* **2000**, *112*, 7089.
- Zhou, M. F.; Zhang, L. N.; Qin, Q. *Z. J. Am. Chem. Soc.* **2000**, *122*, 4483.